

Extreme Compression of Adaptive Neural Images

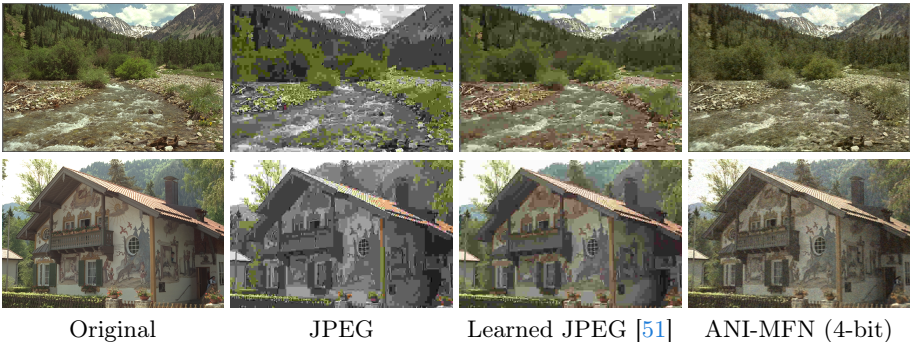
Leo Hoshikawa^{*1}, Marcos V. Conde^{*2}, Takeshi Ohashi¹, and Atsushi Irie¹

¹ Sony Group Corporation

² Sony PlayStation, VCG, FTG

Abstract. Implicit Neural Representations (INRs) and Neural Fields are a novel paradigm for signal representation, from images and audio to 3D scenes and videos. The fundamental idea is to represent a signal as a continuous and differentiable neural network. This idea offers unprecedented benefits such as continuous resolution and memory efficiency, enabling new compression techniques. However, representing data as neural networks poses new challenges. For instance, given a 2D image as a neural network, how can we further compress such a neural image?. In this work, we present a novel analysis on compressing neural fields, with the focus on images. We also introduce Adaptive Neural Images (ANI), an efficient neural representation that enables adaptation to different inference or transmission requirements. Our proposed method allows to reduce the bits-per-pixel (bpp) of the neural image by 4x, without losing sensitive details or harming fidelity. We achieve this thanks to our successful implementation of 4-bit neural representations. Our work offers a new framework for developing compressed neural fields.

Keywords: Image Compression · Implicit Neural Representations · Machine Learning · Neural Networks · Neural Fields



Original

JPEG

Learned JPEG [51]

ANI-MFN (4-bit)

Fig. 1: Comparison with traditional codecs. Our proposed neural image ANI (at 4-bits) achieves high-fidelity results without clearly unpleasant artifacts. Note that all the images are around 0.3 bpp. The images from the Kodak dataset are: 13 and 24.

^{*} equal contribution

1 Introduction

Neural fields, also known as Implicit Neural Representations (INRs), allow the representation of signals (or data) of all kinds and have emerged as a new paradigm in the field of signal processing, neural compression, and neural rendering [19, 36, 47, 50, 55]. Unlike traditional discrete representations (*e.g.* an image is a discrete grid of pixels, audio signals are discrete samples of amplitudes), neural fields are continuous functions that describe the signal. Such a function maps the source domain \mathcal{X} of the signal to its characteristic values \mathcal{Y} . For instance, it can map 2D pixel coordinates to their corresponding RGB values in the image $\mathcal{I}[x, y]$. This function ϕ is approximated using neural networks (NNs), thus it is continuous and differentiable. We can formulate this as

$$\phi : \mathbb{R}^2 \mapsto \mathbb{R}^3 \quad \mathbf{x} \rightarrow \phi(\mathbf{x}) = \mathbf{y}, \quad (1)$$

where ϕ is the learned INR function, the domains $\mathcal{X} \in \mathbb{R}^2$ and $\mathcal{Y} \in \mathbb{R}^3$, the input coordinates $\mathbf{x} = (x, y)$, and the output RGB value $\mathbf{y} = [r, g, b]$. In summary, neural representations are essentially simple neural networks (NNs), once these networks ϕ (over)fit the signal, they become implicitly the signal itself.

This approach has become foundational research in many areas including image compression [19, 20, 50], audio compression [52, 53], video compression [12, 14] and 3D representations (*e.g.* NeRF, DeepSDF) [36, 38, 40, 41].

In the context of *image compression*, this method offers unique mathematical properties due to its continuous and differentiable nature [19, 20, 50]. One of the major advantages of using INRs is that they are not tied to spatial resolution. Unlike conventional methods where the image resolution is tied to the discrete number of pixels, the memory needed for these representations only scales with the complexity of the underlying signal [47, 55]. In essence, they offer “infinite resolution”, meaning they can be sampled at any spatial resolution [47] by upsampling the input domain \mathcal{X} (*e.g.* $[H, W]$ grid of coordinates). This makes them particularly useful for high-dimensional signal parameterization, where traditional methods struggle due to memory limitations.

Considering this, we define a *neural image* as a neural network (INR) that represents a particular image of an arbitrary resolution — see Figure 2.

Recent works [19, 20, 38] demonstrates that we can fit large images (even gigapixel images) using “small” neural networks as INRs, which implies promising compression capabilities [19, 20]. These seminal works [19, 50] show that INRs can be a better option than standard image codecs such as JPEG [42] and JPEG2000 [49] in the following scenarios: (i) high-resolution images, (ii) extreme compression at low bits-per-pixel (bpp). However, neural fields represent a *lossy compression* technique, specially limited by Shannon’s Theorem [46] *i.e.* even utilizing complex deep neural networks, to parameterize the high-frequencies of certain images remains a challenging or impossible task.

In this work, we focus on the particular case of 2D images, since it is well-known that this serves as a good proxy for 3D research [36, 47, 48, 55].

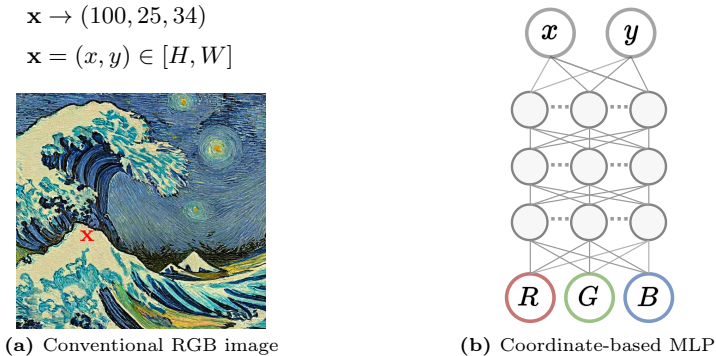


Fig. 2: We illustrate the general concepts around neural image representations [47, 55]. INRs can be generalized to other sort of signals such as audio or 3D representations.

Contributions (i) We provide an extensive benchmark on extreme image compression using neural fields. (ii) We propose Adaptive Neural Images (ANI), a novel neural representation that allows adaptation to different memory and inference requirements. We achieve this by using *state-of-the-art* neural architecture search (NAS) to find the optimal neural network. Our approach allows to reduce $4\times$ the required bits-per-pixel without losing much fidelity. (iii) We provide useful insights related to the quantization of neural fields, that can be applied to other related tasks (*i.e.* 3D NeRF).

2 Related Work

Learned Image Compression. The concept of learned image compression was pioneered by [4], through the introduction of an end-to-end framework combining an auto-encoder with an entropy model to jointly optimize both rate and distortion metrics. Many approaches [5, 32, 34, 37] enhanced this model by incorporating a scaling hyper-prior to the architecture, and the use of autoregressive entropy models. The current trend on generative image compression represents the state-of-the-art in terms of perceptual quality [2, 3, 27, 35].

Model Compression. Due to the industry requirements in terms of inference speed, memory and energy consumption, in the recent years there has been plenty of research on model compression [16, 33, 59]. For instance, [26] proposes a simple framework: applying pruning, quantization and entropy coding –in sequence– combined with retraining in between the steps. To optimize performance under quantization, several works use mixed-precision quantization and post-quantization optimization techniques [11, 15, 17, 21, 39, 56, 57].

We find particularly useful LSQ+ [7], which improves low-bit quantization through learnable offsets and better initialization.

In the context of neural fields, the neural network represents the data itself, thus, model compression implies (additional) data compression. Despite this seems a promising approach, very few works tackle this problem [25].

Neural Architecture Search (NAS) In the recent years, Neural Architecture Search (NAS) has emerged as a powerful approach for automating the design of optimal neural network architectures for a given task, significantly reducing the need for manual experimentation [62, 63]. The field has since seen rapid progress, with methods like Efficient Neural Architecture Search (ENAS) by Pham et al. [43], which significantly reduces search time by sharing weights among different architectures. Once-for-All [10] allows to train a single neural network and specialize it for efficient deployment.

2.1 Neural Representations

In recent years, implicit neural representations (INRs) [18, 23, 38, 47] have become increasingly popular in image processing as a novel way to parameterize an image. Also known as coordinate-based networks, these approaches use multilayer perceptrons (MLPs) to overfit to the image, and thus, represent it. Multiple works have demonstrated the potential of MLPs as continuous, memory-efficient implicit representations for images [47, 50]; we find especially inspiring SIREN [47].

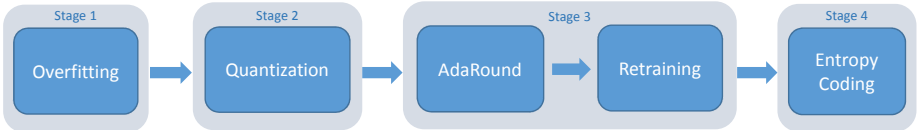
We denote the INRs as a function ϕ with parameters θ , defined as:

$$\begin{aligned}\phi(\mathbf{x}) &= \mathbf{W}_n(\varsigma_{n-1} \circ \varsigma_{n-2} \circ \dots \circ \varsigma_0)(\mathbf{x}) + \mathbf{b}_n \\ \varsigma_i(x_i) &= \alpha(\mathbf{W}_i \mathbf{x}_i + \mathbf{b}_i),\end{aligned}\tag{2}$$

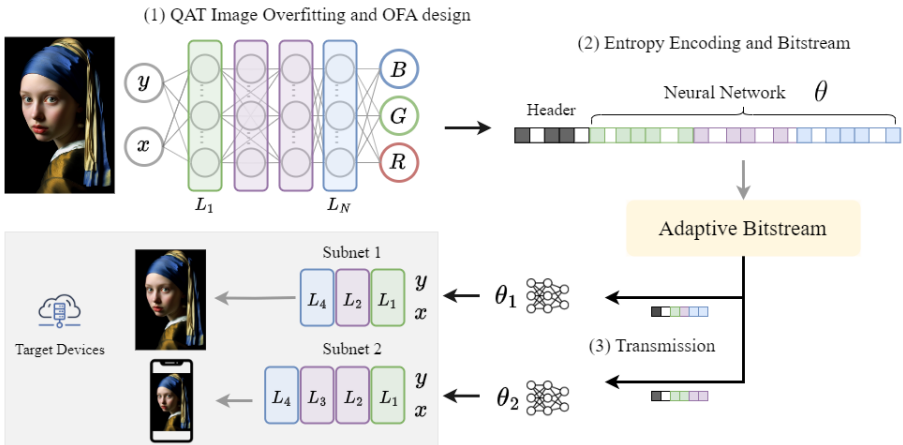
where ς_i are the layers of the network (considering their corresponding weight matrices \mathbf{W} and bias \mathbf{b}), and α is a nonlinear activation *e.g.* ReLU, Tanh, Sine [47], complex Gabor wavelet [44]. Considering this formulation, the parameters of the neural network θ is the set of weights and biases of each layer (*i.e.* \mathbf{W} and \mathbf{b}). Since the input of the MLP are the coordinates \mathbf{x} in the domain $[H, W] \in \mathbb{R}^2$, these are also known as coordinate-based MLPs — see Figure 2b.

Sitzmann *et al.* [47] presented SIREN, a periodic activation function for neural networks based on the Sine function, specifically designed to better model complex natural signals and high-frequencies in the images. Tancik *et al.* [55] introduced fourier features as input positional encodings for the network, enhancing their capability to model high-frequencies. COIN [19, 20] explored the early use of INRs for image compression. Strumpler *et al.* [50] proposed a framework for image compression and transmission using INRs. We also find other works that tackle new activation functions such as multiplicative filter networks (MFN) [22] and Wire [44], and multi-scale representations [38, 45]. Other such as Instant-NGP [38] and SHACIRA [24] approaches focus on multi-resolution representations using hierarchical representations and hash-tables to improve performance and speed.

Following previous work [19, 50], we will use SIREN [47] as the baseline model. We will explore extreme compression of the neural network, and new training techniques to derive our proposed adaptive neural images (ANI). We will also analyze the most popular and recent approaches: FourierNets [55] (MLP with Positional Encoding), SIREN [47], MFN [22], Wire [44] and DINER [60].



(a) Overview of INR-based compression pipeline proposed by Y. Strümpler et al. [50]. The basic compression pipeline comprises image overfitting, quantization of the neural network, AdaRound, retraining and lossless entropy coding (*e.g.* binarized arithmetic coding).



(b) Our proposed approach using adaptive neural images (ANI). We perform directly quantization aware training (QAT) [7] and once-for-all (OFA) optimization [10]. Depending on the bandwidth and transmission requirements, our bitstream can be adapted (*e.g.* trimmed) allowing to send more/less information, this is only possible thanks to the proposed ANI architecture. Moreover, depending on the target device speed and memory requirements, we can utilize smaller versions of our neural network ANI without any re-training or adaptation. We highlight the client side and target devices.

Fig. 3: We illustrate the general concepts around image compression and transmission using INRs [50]. Our approach enables to adapt to diverse scenarios depending on the bandwidth, memory, and target device requirements.

3 Transmission of Neural Images

Transmitting signals as INRs is a novel research problem [20, 50]. In this context, it is fundamental to understand that the image is no longer characterized as a discrete set of RGB pixels, but as a set of weights and biases (θ *i.e.* the neural network itself). We illustrate in Figure 3a the most popular approach for compressing images using INRs. First, we train the neural network ϕ to fit the image, next we can apply post-training quantization (PTQ) and encode the parameters θ using lossless entropy coding. We could also apply post-quantization retraining to improve the performance of the neural network. Finally we can transmit the parameters θ , the client can recover the network, and thus reconstruct the natural RGB image.

Our approach considers quantization aware training (QAT) directly, which offers better performance. We show our method in Figure 3b.

Besides QAT, the key concept of our approach is the active neural architecture search (NAS) to produce a “once-for-all” neural network [10] *i.e.* a single network is trained to support versatile architectural configurations including depth (number of layers) and width (number of neurons). Therefore considering our neural image with parameters θ we can derive –during inference– different sub-networks with varying number of layers and neurons. We illustrate the sub-networks θ_1 and θ_2 in Figure 3b.

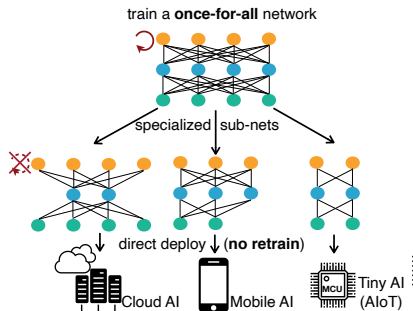


Fig. 4: Once-for-all (OFA) [10] networks allow to get specialized sub-network for different requirements.

We define **adaptive neural images (ANIs)** as a once-for-all neural representations of images. Note that ANIs are also trained to support quantization. Note that the neural representation training is done *offline* only once for a particular image, thus, the training time is not a constrained. Moreover, training to convergence is possible in a few minutes.

Meta-learning Strümpler et al. [50] proposes to use a fixed meta-INR as initialization θ^* , and adjust (fine-tune) the network to the desired image to obtain θ . Next we transmit only a residual $\Delta\theta = \theta - \theta^*$. Such a sparse representation of the neural network allows to simplify the transmitted information and make the process more efficient [50]. Finally the client recovers the INR knowing $\Delta\theta$ and the θ^* (meta-INR), and reconstructs the natural image. This technique is a research topic by itself [13, 31, 54], for this reason, we do not use meta-learning in our experiments and we focus on neural models compression.

General Limitations Before presenting our approach, we must discuss the fundamental limitations of neural images to better understand the experimental results. First, INRs are a lossy compression method. Second, most INR approaches are signal-specific *i.e.* the neural network fits a particular image. This implies training *ad hoc* the neural network using a GPU — although this can take less than 1 minute, and meta-learning [54] helps to accelerate training. Third, the performance of the INR methods highly varies depending on hyper-parameters (*e.g.* learning rate, number of neurons and layers), and the target signal. However, there is no theoretical or practical way of predicting *a priori* which INR model fits best the signal.

4 Our Approach for Extreme Compression

Given a neural representation of an image –a neural image–, our goal is to reduce as much as possible the number of bits while preserving the original

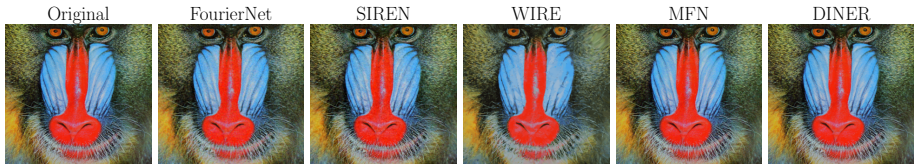


Fig. 5: Results on the image baboon using state-of-the-art INRs [22, 44, 47, 55, 60].

Method	Param. (K)	PSNR \uparrow	SSIM \uparrow
FourierNet [55]	66.30	27.05 \pm 1.33	0.750
SIREN [47]	66.82	27.98 \pm 2.73	0.782
MFN [22]	70.27	29.16 \pm 2.80	0.822
Wire [44]	66.82	25.96 \pm 3.83	0.712
DINER [60]	545.55	27.34 \pm 15.5	0.751

Table 1: Comparison of *state-of-the-art* INRs on the Kodak dataset [1]. We report the average PSNR (\pm std.) and SSIM [58] over 5 runs. We observe high variability in DINER [60]. The neural networks have 4 layers, each with 128 neurons.

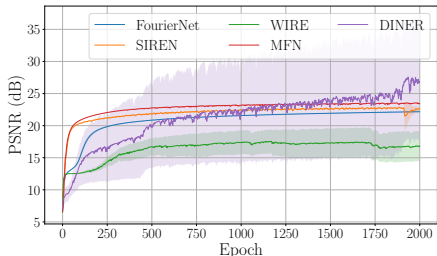


Table 2: Samples of training evolution of the different INR methods [22, 44, 47, 55, 60]. This corresponds to baboon. We show the average results over 5 runs, and its corresponding confidence interval.

signal. Considering that the neural network represents the signal itself, we must focus on compressing the neural network (*i.e.* weights and biases).

4.1 Selecting the Neural Model

First, we analyze the current *state-of-the-art* of INRs and their limitations. Although INRs are popular for image compression, to the best of our knowledge there is not any benchmark comparing their performance beyond single images.

We compare FourierNets [55] (MLP with Positional Encoding), SIREN [47], MFN [22], Wire [44] and DINER [60] using well-known dataset for image processing. We show a visual comparison in Figure 5.

We conduct an exhaustive study using the well-known Kodak dataset [1]. We present the results in Table 1. From this experiment we can conclude: (i) the performance of an INR highly depends on the target image. (ii) Given an image, the performance of an INR can vary notably due to the random initialization – for this reason we repeat each training 5 times with different random seeds. (iii) As we show in Figure 2, the training –overfitting– can be highly unstable depending on the model (*e.g.* DINER [60]). We provide more training samples in the appendix.

The particular case of DINER [60] (*CVPR '23*) suggests that using non-differentiable hash-tables difficulties training.

Considering the experiment and conclusions, we decide to use mainly SIREN [47] and MFN [22] in our compression analysis because of the following reasons: (i)

the models offer stable performance and good fidelity, (ii) do not require non-differentiable hash tables, (iii) their non-linear activations facilitate advanced quantization due to their mathematical properties.

4.2 Post-Training Quantization

Post-Training Quantization (PTQ) calculates quantization parameters without re-training. On our experiments we adopted the standard PTQ algorithm proposed by [28] and used as standard on several studies [50]. This algorithm allows to quantize models to 7-bits and 8-bits.

4.3 Quantization-Aware Training (QAT)

Quantization-aware training (QAT) methods have a considerable advantage over PTQ methods in terms of compression ratio [8, 21, 26, 29], allowing extremely small bit-width (2, 4-bit) at the expense of additional training time.

In general neural networks, weights follow zero-mean normal distributions, while the distribution for the activations varies greatly depending on the architecture and non-linearities. For INRs, the behaviour of the MLP and activations is well-known. In SIREN [47] the sine activation conveniently restricts the distribution to a normalized range with zero-mean. For MFNs [22], the filter passes through the sine activation and are multiplied by the output of the linear layers, conveniently restricting the range. These properties allow us to experiment extreme compression at low-bit (4,8-bit) or ternary quantization.

Unlike previous methods [25, 50], we use the *state-of-the-art* LSQ+ [8] quantization algorithm. We adapt this algorithm for INRs as follows:

Algorithm 1 Quantization-Aware Training using Learnable Step Size Quantization (LSQ/LSQ+)

Require: Input tensor X , number of bits b , learnable step size s

Ensure: Quantized tensor Q

$Q_{\max} \leftarrow 2^{b-1} - 1$

$Q_{\min} \leftarrow -2^{b-1}$

// Forward pass quantization

$X_{\text{scaled}} \leftarrow X/s$

$X_{\text{clipped}} \leftarrow \max(\min(X_{\text{scaled}}, Q_{\max}), Q_{\min})$

$Q \leftarrow \text{round}(X_{\text{clipped}})$

// During backpropagation, update s using gradient descent

return $Q \times s$ {Return de-quantized tensor for subsequent computations}

Following the notation from [7], we define \bar{x} and \hat{x} as the coded bits and quantized values, respectively. The weights are quantized as follows:

$$\bar{x} = \text{quantize}(\text{clamp}(\frac{x}{s}, -1, 1)) \quad \text{and} \quad \hat{x} = \bar{x} \times s \quad (3)$$

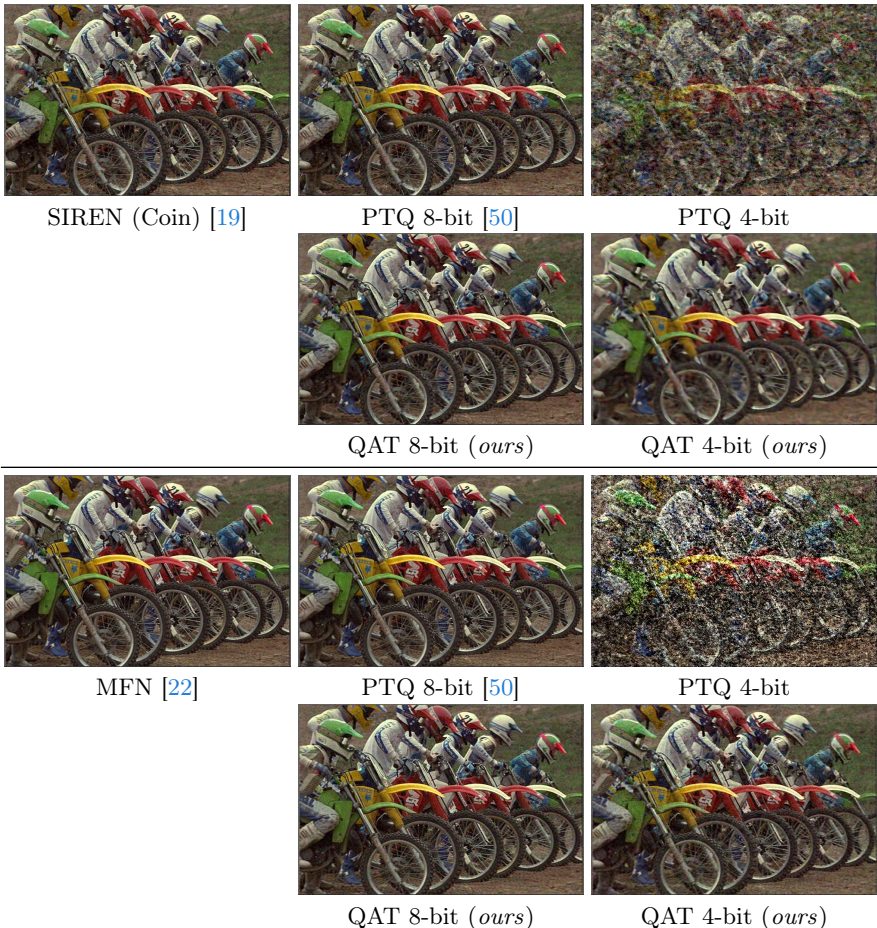


Fig. 6: Comparison between PTQ and QAT. Visual results on Kodak [1] at different bit-widths. We can appreciate how at 4-bits PQT loses the signal, while QAT maintains high fidelity. Our method improves previous approaches [19, 20, 50].

Meanwhile, for the activations we use the following function:

$$\bar{x} = \text{quantize}(\text{clamp}(\frac{x - \beta}{s}, -1, 1)) \quad \text{and} \quad \hat{x} = \bar{x} \times s + \beta \quad (4)$$

Where the parameters s and β are learned using back-propagation [7] *i.e.* a learned affine transformation. On 8-bits quantization is given by:

$$\bar{x} = \frac{\text{round}((\bar{x} + 1) \times 2^{b-1})}{2^b} \quad \text{where } b \text{ is the number of bits.} \quad (5)$$

The same equation is applied to both the weights and activations. We used straight-through estimator (STE) [6] and update the quantization parameters

using backpropagation. In Figure 6 we show the benefits of using LSQ+ [7] quantization aware training (QAT) instead of post-training quantization (PTQ).

4.4 Neural Architecture Search (NAS)

We experimented with NAS to find optimal architectures automatically. Since we expect multiple target devices and different specifications, we use Once-for-All (OFA) [9], a supernet approach that allows training once and obtain multiple sub-architectures with minimal retraining, and adapted to INRs. Since INRs are essentially MLPs, the only parts that we can make “elastic” are the depth (number of layers) and the width (number of channels or neurons). Additionally, in order to simplify the search space, we adopted uniform number of channels per layer. This restricted the search space, and allows us to train and evaluate several possible layouts.

During training, the subnets are initialized using progressive shrinking proposed by OFA [9]. we alternate between large and small networks to remove architecture related bias, inspired the sandwich rule proposed by [61]. Next, we fine-tune the sub-networks for a small amount of epochs to improve the fidelity *w.r.t* the target image.

Algorithm 2 Once-for-all training strategy

Require: Search space of channels $W=\{W_0, W_1, \dots, W_n\}$, layers $D=\{D_0, D_1, \dots, D_n\}$

```

 $S = W \times D$ 
for each  $s \in S$  do
  params = get_model_size(s)
end for
//Argsort S using params
 $idx = \text{argsort}(params)$ 
//Reorder S by alternating large and small architectures
 $S_{sorted} = \text{sort\_and\_shuffle}(S, idx)$ 
 $supernet = \text{build\_model}(W_n, D_n)$ 
train(supernet)
for each  $s \in S_{sorted}$  do
  subnet = supernet.get_subnet(s)
  train(subnet)
end for
return subnet

```

5 An INR Compression Benchmark

We build an exhaustive benchmark using the Kodak dataset [1], we provide the results in Table 3. Each experiment was repeated five times with different random seeds. We report the average performance of the five experiments. In all the experiments we use models with 4 layers and 128 channels.

Method	Quantization	Size(KB)	PSNR \uparrow	SSIM \uparrow	BPP \downarrow
SIREN [47]	Coin [19] (None)	270.28	27.98 \pm 2.73	0.782	1.812
	PTQ 8-bit [50]	71.46	27.78 \pm 2.71	0.760	0.479
	PTQ 4-bit (<i>ours</i>)	38.33	18.24 \pm 1.72	0.216	0.257
	QAT 8-bit (<i>ours</i>)	71.46	27.26 \pm 2.74	0.742	0.479
	QAT 4-bit (<i>ours</i>)	38.33	25.35 \pm 2.73	0.638	0.257
MFN [22]	Coin [19] (None)	284.29	29.16 \pm 2.80	0.822	1.906
	PTQ 8-bit [50]	85.43	28.60 \pm 2.82	0.785	0.572
	PTQ 4-bit (<i>ours</i>)	52.29	14.22 \pm 2.20	0.136	0.350
	QAT 8-bit (<i>ours</i>)	85.43	28.61 \pm 2.60	0.780	0.572
	QAT 4-bit (<i>ours</i>)	52.30	26.79 \pm 2.33	0.683	0.350

Table 3: Quantization INR Analysis on Kodak [1]. We report the average PSNR –over 5 runs– for the whole Kodak image dataset using different quantization settings. All the neural networks have 4 layers and 128 neurons. We are the first approach to achieve successfully 4-bit quantization of neural images.

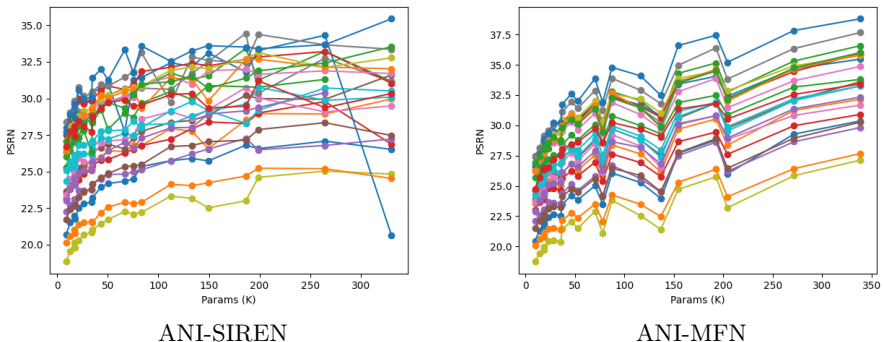


Fig. 7: Building ANIs. We use OFA [9] to build our adaptive neural images (ANIs). We show the PSNR for different models of the OFA super-network’s search space. Each color represents an image form Kodak dataset. Outliers are due to the unstable training. We can also conclude that deeper networks are better than wider.

For the PTQ experiments we follow [50]. Since the results for this technique are deterministic, we select the best performing model per image (considering the five different runs). Following other quantization experiments, we kept the first and last layers in full precision. The impact of quantizing these layers is described as an ablation study.

To develop our adaptive neural images (ANIs) we use OFA [9]. Using this NAS technique we define our search space of [64, 128, 192, 256] channels and [2, 3, 4, 5] intermediate layers. We train all possible combinations (16 architectures) for 1000 epochs. We show the results of this search in Figure 7.

Benchmark Conclusions Considering the results from Table 3, we are the first approach to achieve successfully 4-bit quantization of neural representations. At 8-bits, both PTQ and QAT provide similar quality without notable degradations. However, at 4-bits, the model quantized with PTQ loses the signal information, yet the model quantized with QAT maintains the signal and provides good fidelity. Our approaches improves Coin [19] and previous INR compression [50] by +7dB in the scenario of 4-bits. Figure 6 shows the visual results. Both SIREN [47] and MFN [22] presented similar behavior during quantization, although SIREN [47] is slightly more cost-efficient due to having less full precision parameters. In Figure 8 we show the results of our ANI *i.e.* a single super-network that allows to infer using sub-networks depending on the memory requirements. We provide more qualitative samples in the appendix.

Ablation Study on Depth-wise Quantization (DwQ).

Table 4 shows the impact of quantizing the first layer (filters for MFN) or the last layers. Quantizing the first layers drops the performance considerably with small compression in exchange, making it cost-ineffective. On the other hand, quantizing the final layer has barely no impact in the quality. See visual results in Figure 9.

Method	PSNR \uparrow	SSIM \uparrow	BPP \downarrow
SIREN [47]	27.73 \pm 0.14	0.771	1.833
8-bit QAT default	26.59 \pm 0.50	0.729	0.479
+ 8-bit first layer	23.74 \pm 0.29	0.587	0.474
+ 8-bit last layer	26.25 \pm 0.54	0.715	0.471
MFN [22]	28.49 \pm 0.23	0.804	1.928
8-bit QAT default	28.72 \pm 0.05	0.782	0.572
+ 8-bit filters	25.10 \pm 0.18	0.666	0.546
+ 8-bit last layer	28.42 \pm 0.12	0.764	0.565

Table 4: Impact of layer quantization.

5.1 Implementation Details

We implement all the methods in PyTorch, using the author’s implementations when available. We train all the models using the same environment with the Adam [30] optimizer, and we adapt the learning rate for each method’s requirements. For instance MFN [22] uses 0.01 while SIREN [47] uses 0.001.

We use NVIDIA RTX 2080Ti cards. The models are optimized using the \mathcal{L}_2 reconstruction loss [47, 55] to minimize the RGB image reconstruction error $\sum_{x,y} \|\mathcal{I}[x,y] - \phi(x,y)\|_2^2$, $\forall(x,y) \in [H,W]$.

Note that due to the memory requirements of FHD images, the optimization is only possible on GPU cars with > 40Gbs of VRAM.

Limitations. A clear limitation of using INRs for neural image compression is their stochastic nature and unstable training. Moreover there is no practical way of predicting *a priori* which INR model fits best the signal. We compare our approach with other compression methods in Figure 10. Our approach represent the most competitive INR solution.

Besides 4-bit quantization, we also experimented with ternary quantization, however the results were not satisfactory. We provide this analysis in the supplementary material.

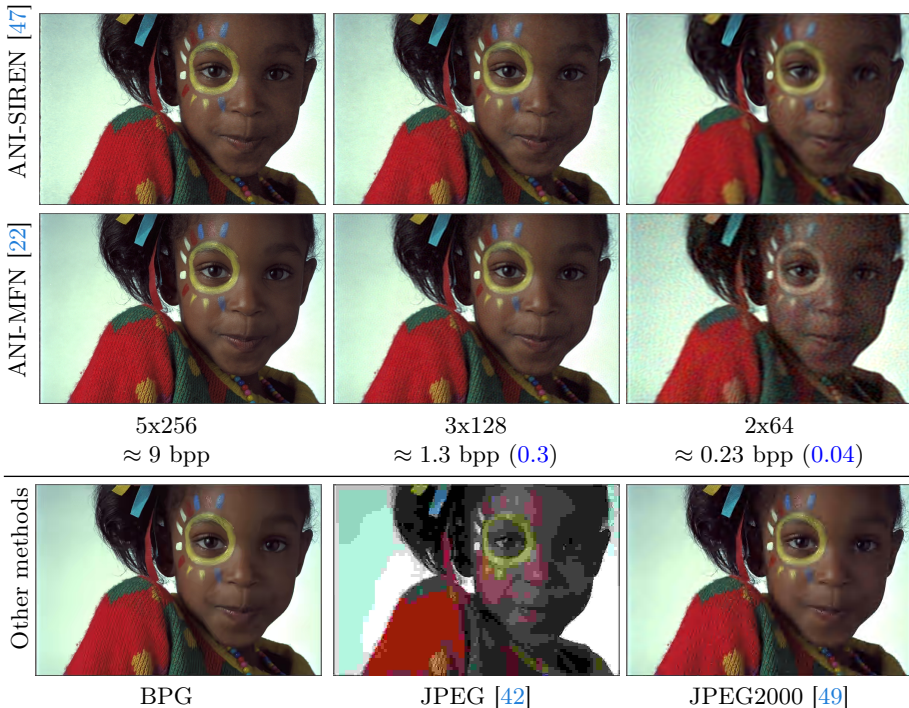


Fig. 8: We present results of ANI with SIREN [47] and MFN [22] as backbones. Our single neural image can be adapted to different memory-fidelity requirements. The images correspond to a single neural network with three different subnetworks defined as layers \times neurons. Our methods achieve better performance than BPG, JPEG [42], JPEG2000 [49] at ≈ 0.23 bpp. We indicate in blue the approximated 4-bit bpp. Note that these ANI models are not quantized.

6 Conclusion

In this work, we present a novel analysis on compressing neural representations. We also introduce Adaptive Neural Images (ANI), an efficient neural representation that enables adaptation to different inference or transmission requirements. We derive our ANI super-network using advanced once-for-all architecture search. To the best of our knowledge, we are the first approach to achieve successfully 4-bit quantization of neural representations. Moreover, this work provides the most complete benchmark for this task. Our work offers a transversal framework for developing compressed neural fields.

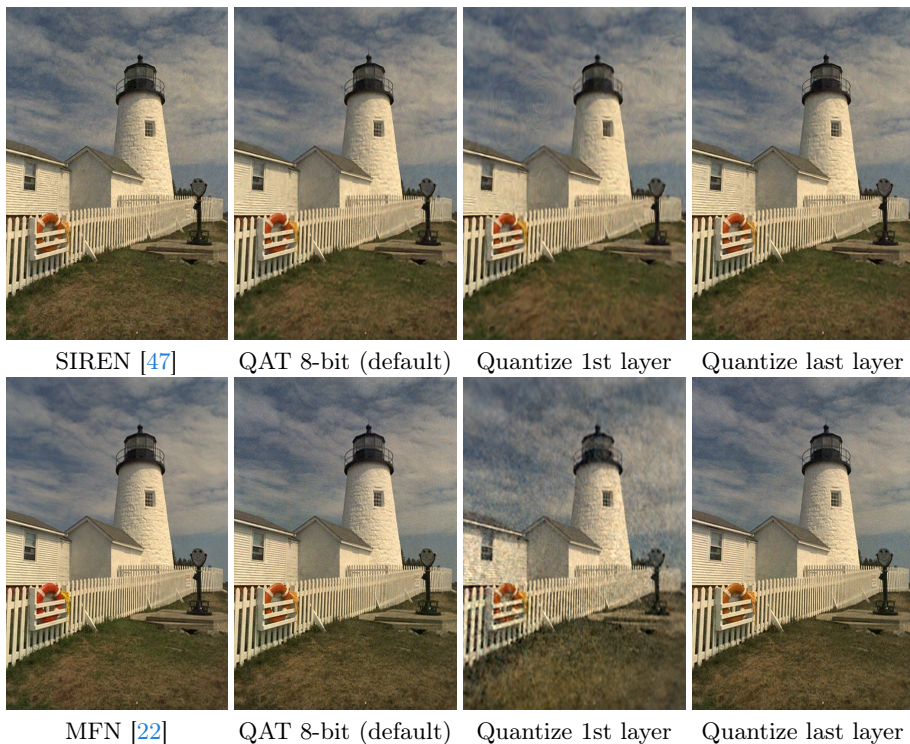


Fig. 9: Ablation study for depth-wise quantization. We can appreciate the negative effects of quantizing the early layers, in contrast, quantizing the last layer does not affect much the fidelity. This denotes the importance of the first layers (or filters).

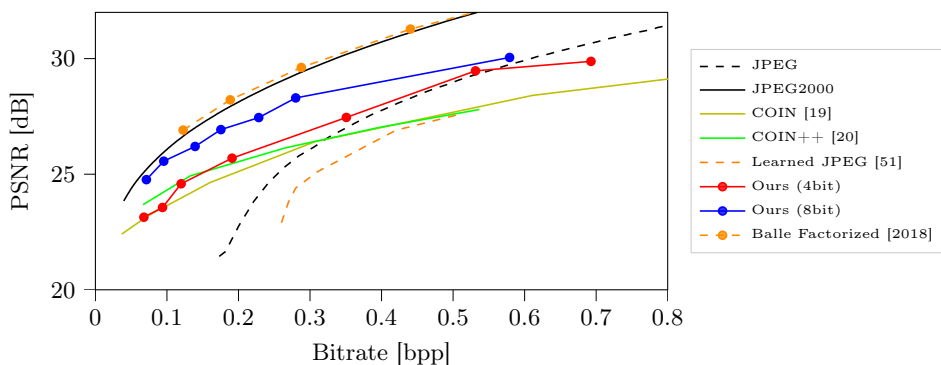


Fig. 10: Comparison of our approach on the Kodak dataset with other methods. Note that ANI-MFN is a single neural network that can be adapted to different bpp requirements, unlike Coin [19, 20] or SIREN [47, 50].

References

1. Kodak lossless true color image suite. <http://r0k.us/graphics/kodak/> **7, 9, 10, 11, 19**
2. Agustsson, E., Minnen, D., Toderici, G., Mentzer, F.: Multi-realism image compression with a conditional generator. In: Proceedings of the IEEE/CVF Conference on Computer Vision and Pattern Recognition. pp. 22324–22333 (2023) **3**
3. Agustsson, E., Tschannen, M., Mentzer, F., Timofte, R., Gool, L.V.: Generative adversarial networks for extreme learned image compression. In: Proceedings of the IEEE/CVF International Conference on Computer Vision (ICCV). pp. 221–231 (2019) **3**
4. Ballé, J., Laparra, V., Simoncelli, E.P.: End-to-end optimized image compression. International Conference on Learning Representations (ICLR) (2017) **3**
5. Ballé, J., Minnen, D., Singh, S., Hwang, S.J., Johnston, N.: Variational image compression with a scale hyperprior. International Conference on Learning Representations (ICLR) (2018) **3**
6. Bengio, Y., Léonard, N., Courville, A.: Estimating or propagating gradients through stochastic neurons for conditional computation. arXiv preprint arXiv:1308.3432 (2013) **9**
7. Bhalgat, Y., Lee, J., Nagel, M., Blankevoort, T., Kwak, N.: Lsq+: Improving low-bit quantization through learnable offsets and better initialization. In: Proceedings of the IEEE/CVF Conference on Computer Vision and Pattern Recognition Workshops. pp. 696–697 (2020) **3, 5, 8, 9, 10**
8. Bhalgat, Y., Lee, J., Nagel, M., Blankevoort, T., Kwak, N.: LSQ+: improving low-bit quantization through learnable offsets and better initialization. CoRR **abs/2004.09576** (2020), <https://arxiv.org/abs/2004.09576> **8**
9. Cai, H., Gan, C., Han, S.: Once for all: Train one network and specialize it for efficient deployment. CoRR **abs/1908.09791** (2019), <http://arxiv.org/abs/1908.09791> **10, 11**
10. Cai, H., Gan, C., Wang, T., Zhang, Z., Han, S.: Once-for-all: Train one network and specialize it for efficient deployment. arXiv preprint arXiv:1908.09791 (2019) **4, 5, 6**
11. Chai, S.M.: Quantization-guided training for compact TinyML models. Research Symposium on Tiny Machine Learning (2021) **3**
12. Chen, H., He, B., Wang, H., Ren, Y., Lim, S.N., Shrivastava, A.: Nerv: Neural representations for videos. Advances in Neural Information Processing Systems **34**, 21557–21568 (2021) **2**
13. Chen, Y., Wang, X.: Transformers as meta-learners for implicit neural representations. In: European Conference on Computer Vision. pp. 170–187. Springer (2022) **6**
14. Chen, Z., Chen, Y., Liu, J., Xu, X., Goel, V., Wang, Z., Shi, H., Wang, X.: Videoinr: Learning video implicit neural representation for continuous space-time super-resolution. In: Proceedings of the IEEE/CVF Conference on Computer Vision and Pattern Recognition. pp. 2047–2057 (2022) **2**
15. Choukroun, Y., Kravchik, E., Yang, F., Kisilev, P.: Low-bit quantization of neural networks for efficient inference. In: 2019 IEEE/CVF International Conference on Computer Vision Workshop (ICCVW). pp. 3009–3018. IEEE (2019) **3**
16. Dettmers, T., Pagnoni, A., Holtzman, A., Zettlemoyer, L.: Qlora: Efficient fine-tuning of quantized llms. Advances in Neural Information Processing Systems **36** (2024) **3**

17. Dong, Z., Yao, Z., Gholami, A., Mahoney, M.W., Keutzer, K.: Hawq: Hessian aware quantization of neural networks with mixed-precision. *International Conference on Computer Vision (ICCV)* (2019) [3](#)
18. Dou, Y., Zheng, Z., Jin, Q., Ni, B.: Multiplicative fourier level of detail. In: *Proceedings of the IEEE/CVF Conference on Computer Vision and Pattern Recognition*. pp. 1808–1817 (2023) [4](#)
19. Dupont, E., Goliński, A., Alizadeh, M., Teh, Y.W., Doucet, A.: Coin: Compression with implicit neural representations. *arXiv preprint arXiv:2103.03123* (2021) [2](#), [4](#), [9](#), [11](#), [12](#), [14](#), [19](#), [20](#), [21](#)
20. Dupont, E., Loya, H., Alizadeh, M., Goliński, A., Teh, Y.W., Doucet, A.: Coin++: Neural compression across modalities. *arXiv preprint arXiv:2201.12904* (2022) [2](#), [4](#), [5](#), [9](#), [14](#), [19](#)
21. Esser, S.K., McKinstry, J.L., Bablani, D., Appuswamy, R., Modha, D.S.: Learned step size quantization. *arXiv preprint arXiv:1902.08153* (2019) [3](#), [8](#)
22. Fathony, R., Sahu, A.K., Willmott, D., Kolter, J.Z.: Multiplicative filter networks. In: *International Conference on Learning Representations* (2020) [4](#), [7](#), [8](#), [9](#), [11](#), [12](#), [13](#), [14](#), [19](#), [20](#)
23. Genova, K., Cole, F., Vlasic, D., Sarna, A., Freeman, W.T., Funkhouser, T.: Learning shape templates with structured implicit functions. In: *ICCV*. pp. 7154–7164 (2019) [4](#)
24. Girish, S., Shrivastava, A., Gupta, K.: Shacira: Scalable hash-grid compression for implicit neural representations. In: *Proceedings of the IEEE/CVF International Conference on Computer Vision*. pp. 17513–17524 (2023) [4](#)
25. Gordon, C., Chng, S.F., MacDonald, L., Lucey, S.: On quantizing implicit neural representations. In: *Proceedings of the IEEE/CVF Winter Conference on Applications of Computer Vision*. pp. 341–350 (2023) [3](#), [8](#)
26. Han, S., Mao, H., Dally, W.J.: Deep Compression: Compressing deep neural network with pruning, trained quantization and huffman coding. *International Conference on Learning Representations, (ICLR)* (2016) [3](#), [8](#)
27. Hoogeboom, E., Agustsson, E., Mentzer, F., Versari, L., Toderici, G., Theis, L.: High-fidelity image compression with score-based generative models. *arXiv preprint arXiv:2305.18231* (2023) [3](#)
28. Jacob, B., Kligys, S., Chen, B., Zhu, M., Tang, M., Howard, A.G., Adam, H., Kalenichenko, D.: Quantization and training of neural networks for efficient integer-arithmetic-only inference. *CoRR* [abs/1712.05877](#) (2017), <http://arxiv.org/abs/1712.05877> [8](#)
29. Jain, S., Gural, A., Wu, M., Dick, C.: Trained quantization thresholds for accurate and efficient fixed-point inference of deep neural networks. *Proceedings of Machine Learning and Systems* **2**, 112–128 (2020) [8](#)
30. Kingma, D.P., Ba, J.: Adam: A method for stochastic optimization. *arXiv preprint arXiv:1412.6980* (2014) [12](#)
31. Lee, J., Tack, J., Lee, N., Shin, J.: Meta-learning sparse implicit neural representations. *Advances in Neural Information Processing Systems* **34**, 11769–11780 (2021) [6](#)
32. Lee, J., Cho, S., Beack, S.K.: Context-adaptive entropy model for end-to-end optimized image compression. In: *Proceedings of the International Conference on Learning Representations (ICLR)* (2019) [3](#)
33. Menghani, G.: Efficient deep learning: A survey on making deep learning models smaller, faster, and better (2021) [3](#)

34. Mentzer, F., Agustsson, E., Tschannen, M., Timofte, R., Van Gool, L.: Conditional probability models for deep image compression. In: Proceedings of the IEEE Conference on Computer Vision and Pattern Recognition (CVPR). pp. 4394–4402 (2018) [3](#)
35. Mentzer, F., Toderici, G.D., Tschannen, M., Agustsson, E.: High-fidelity generative image compression. *Advances in Neural Information Processing Systems (NeuIPS)* **33** (2020) [3](#)
36. Mildenhall, B., Srinivasan, P.P., Tancik, M., Barron, J.T., Ramamoorthi, R., Ng, R.: Nerf: Representing scenes as neural radiance fields for view synthesis. *Communications of the ACM* **65**(1), 99–106 (2021) [2](#)
37. Minnen, D., Ballé, J., Toderici, G.: Joint autoregressive and hierarchical priors for learned image compression. *Advances in Neural Information Processing Systems (NeurIPS)* (2018) [3](#)
38. Müller, T., Evans, A., Schied, C., Keller, A.: Instant neural graphics primitives with a multiresolution hash encoding. *ACM Transactions on Graphics (ToG)* **41**(4), 1–15 (2022) [2](#), [4](#)
39. Nagel, M., Amjad, R.A., van Baalen, M., Louizos, C., Blankevoort, T.: Up or down? adaptive rounding for post-training quantization (2020) [3](#)
40. Park, J.J., Florence, P., Straub, J., Newcombe, R., Lovegrove, S.: Deepsdf: Learning continuous signed distance functions for shape representation. In: CVPR (2019) [2](#)
41. Peng, S., Zhang, Y., Xu, Y., Wang, Q., Shuai, Q., Bao, H., Zhou, X.: Neural body: Implicit neural representations with structured latent codes for novel view synthesis of dynamic humans. In: CVPR. pp. 9054–9063 (2021) [2](#)
42. Pennebaker, W.B., Mitchell, J.L.: JPEG: Still image data compression standard. Springer Science & Business Media (1992) [2](#), [13](#), [19](#), [21](#)
43. Pham, H., Guan, M., Zoph, B., Le, Q., Dean, J.: Efficient neural architecture search via parameters sharing. In: International conference on machine learning. pp. 4095–4104. PMLR (2018) [4](#)
44. Saragadam, V., LeJeune, D., Tan, J., Balakrishnan, G., Veeraraghavan, A., Baraniuk, R.G.: Wire: Wavelet implicit neural representations. In: Proceedings of the IEEE/CVF Conference on Computer Vision and Pattern Recognition. pp. 18507–18516 (2023) [4](#), [7](#)
45. Saragadam, V., Tan, J., Balakrishnan, G., Baraniuk, R.G., Veeraraghavan, A.: Miner: Multiscale implicit neural representation. In: European Conference on Computer Vision. pp. 318–333. Springer (2022) [4](#)
46. Shannon, C.E.: Coding Theorems for a Discrete Source With a Fidelity Criterion (1959) [2](#)
47. Sitzmann, V., Martel, J., Bergman, A., Lindell, D., Wetzstein, G.: Implicit neural representations with periodic activation functions. *Advances in neural information processing systems* **33**, 7462–7473 (2020) [2](#), [3](#), [4](#), [7](#), [8](#), [11](#), [12](#), [13](#), [14](#), [19](#), [20](#), [21](#)
48. Sitzmann, V., Zollhoefer, M., Wetzstein, G.: Scene representation networks: Continuous 3d-structure-aware neural. In: *NeurIPS*. vol. 32 (2019) [2](#)
49. Skodras, A., Christopoulos, C., Ebrahimi, T.: The jpeg 2000 still image compression standard. *IEEE Signal processing magazine* **18**(5), 36–58 (2001) [2](#), [13](#)
50. Strümpfer, Y., Postels, J., Yang, R., Gool, L.V., Tombari, F.: Implicit neural representations for image compression. In: European Conference on Computer Vision. pp. 74–91. Springer (2022) [2](#), [4](#), [5](#), [6](#), [8](#), [9](#), [11](#), [12](#), [14](#), [19](#), [21](#)
51. Strümpfer, Y., Yang, R., Timofte, R.: Learning to improve image compression without changing the standard decoder. In: European Conference on Computer Vision. pp. 200–216. Springer (2020) [1](#), [22](#)

52. Su, K., Chen, M., Shlizerman, E.: Inras: Implicit neural representation for audio scenes. *Advances in Neural Information Processing Systems* **35**, 8144–8158 (2022) [2](#)
53. Szatkowski, F., Piczak, K.J., Spurek, P., Tabor, J., Trzciński, T.: Hypersound: Generating implicit neural representations of audio signals with hypernetworks. *arXiv preprint arXiv:2211.01839* (2022) [2](#)
54. Tancik, M., Mildenhall, B., Wang, T., Schmidt, D., Srinivasan, P.P., Barron, J.T., Ng, R.: Learned initializations for optimizing coordinate-based neural representations. In: *Proceedings of the IEEE/CVF Conference on Computer Vision and Pattern Recognition*. pp. 2846–2855 (2021) [6](#)
55. Tancik, M., Srinivasan, P., Mildenhall, B., Fridovich-Keil, S., Raghavan, N., Singhal, U., Ramamoorthi, R., Barron, J., Ng, R.: Fourier features let networks learn high frequency functions in low dimensional domains. *Advances in Neural Information Processing Systems* **33**, 7537–7547 (2020) [2](#), [3](#), [4](#), [7](#), [12](#), [20](#)
56. Uhlich, S., Mauch, L., Cardinaux, F., Yoshiyama, K., Garcia, J.A., Tiedemann, S., Kemp, T., Nakamura, A.: Mixed precision DNNs: All you need is a good parametrization. *International Conference on Learning Representations (ICLR)* (2019) [3](#)
57. Wang, K., Liu, Z., Lin, Y., Lin, J., Han, S.: Haq: Hardware-aware automated quantization with mixed precision. *Conference on Computer Vision and Pattern Recognition (CVPR)* (2019) [3](#)
58. Wang, Z., Bovik, A.C., Sheikh, H.R., Simoncelli, E.P.: Image quality assessment: from error visibility to structural similarity. *IEEE transactions on image processing* **13**(4), 600–612 (2004) [7](#)
59. Xiao, G., Lin, J., Seznec, M., Wu, H., Demouth, J., Han, S.: Smoothquant: Accurate and efficient post-training quantization for large language models. In: *International Conference on Machine Learning*. pp. 38087–38099. PMLR (2023) [3](#)
60. Xie, S., Zhu, H., Liu, Z., Zhang, Q., Zhou, Y., Cao, X., Ma, Z.: Diner: Disorder-invariant implicit neural representation. In: *Proceedings of the IEEE/CVF Conference on Computer Vision and Pattern Recognition*. pp. 6143–6152 (2023) [4](#), [7](#), [20](#)
61. Yu, J., Jin, P., Liu, H., Bender, G., Kindermans, P., Tan, M., Huang, T.S., Song, X., Pang, R., Le, Q.V.: Bignas: Scaling up neural architecture search with big single-stage models. *CoRR* **abs/2003.11142** (2020), <https://arxiv.org/abs/2003.11142> [10](#)
62. Zoph, B., Le, Q.V.: Neural architecture search with reinforcement learning. *arXiv preprint arXiv:1611.01578* (2016) [4](#)
63. Zoph, B., Vasudevan, V., Shlens, J., Le, Q.V.: Learning transferable architectures for scalable image recognition. In: *Proceedings of the IEEE conference on computer vision and pattern recognition*. pp. 8697–8710 (2018) [4](#)

A Supplementary Material

We provide **additional training samples** using the Kodak dataset [1] in Figure 12. As explained in the paper, the most consistent models are SIREN [47] and MFN [22]. For each image we train the models five times and show the average (and std.). This is consistent across the dataset, and justifies our focus on SIREN [47] and MFN [22].

In Figure 13 and Figure 11 we provide high-resolution visual comparisons with previous works. Our approach can capture more high-frequencies and details under extreme compression setups ($< 0.2\text{bpp}$). Moreover, *our ANIs (adaptive neural images) can be adapted to different bpps*, unlike previous methods that are fixed to a particular bpp configuration (changing this would require re-training).

In Figure 10 we extend our distortion-compression plot, focusing on the comparison with previous work COIN (COmpression with Implicit Neural representations) –and related works– [19, 20, 47, 50]. **Our method presents two advantages:** (i) a single model with adaptive bpp capabilities, (ii) improves notably previous approaches and JPEG, specially in extreme compression (very low bpps).

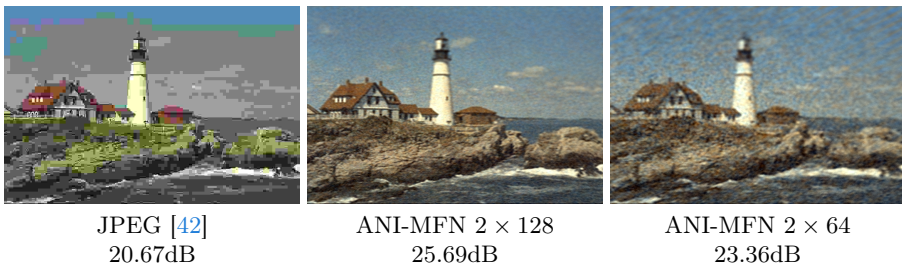


Fig. 11: Comparison of artifacts under extreme compression (< 0.2 bpp). Our ANI-MFN quantized models provide “less harmful” artifacts in comparison with JPEG, for instance we preserve color and structure. Our single model can be adapted to different bpp requirements. In comparison to JPEG (0.17bpp) our smallest model (2 layers, 64 neurons) can provide 0.06bpps .

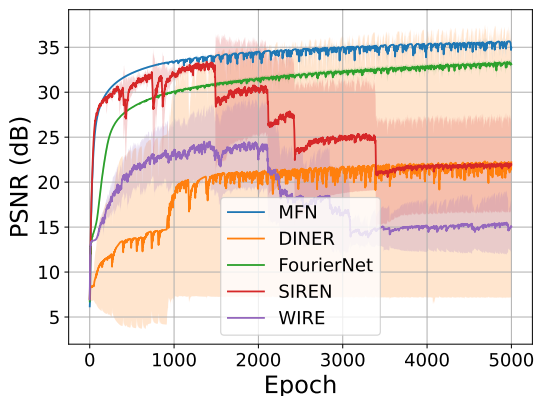
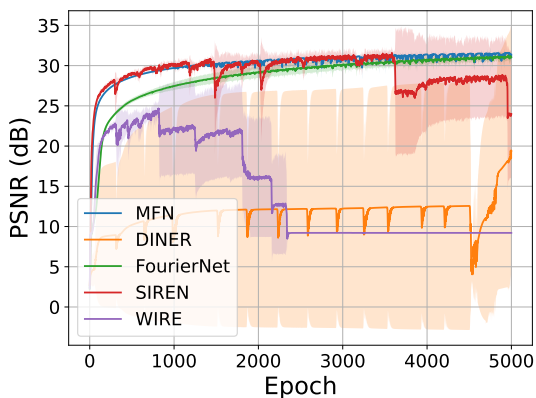
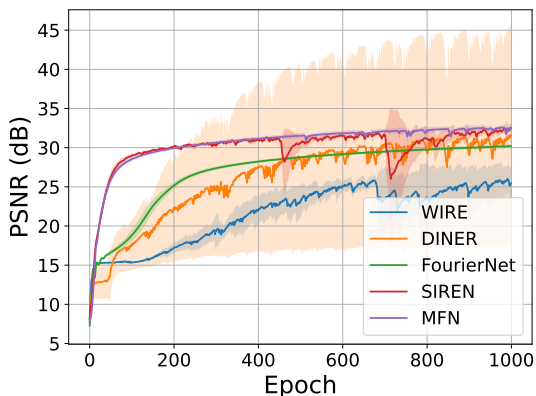


Fig. 12: Comparison of *state-of-the-art* INR backbones for neural image compression [19, 22, 47, 55, 60]. We can appreciate a great *performance variability* depending on the target image. We show the average of 5 experiments (line) and their confidence intervals.

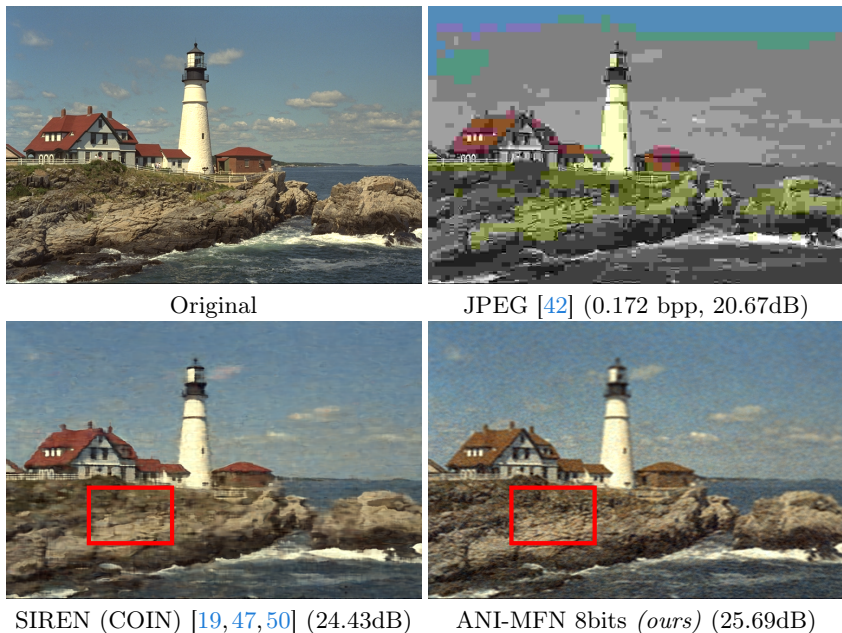


Fig. 13: Comparison with previous works [19, 50] for neural image compression using SIREN [47] as backbone. For a similar range of bpps ≈ 0.17 , both methods provide similar compression capabilities. However, our novel approach ANI allows to adapt to different bpps, while previous works are fixed to a particular bpp. In the highlighted region we can appreciate how our method preserved more high-frequencies and details.

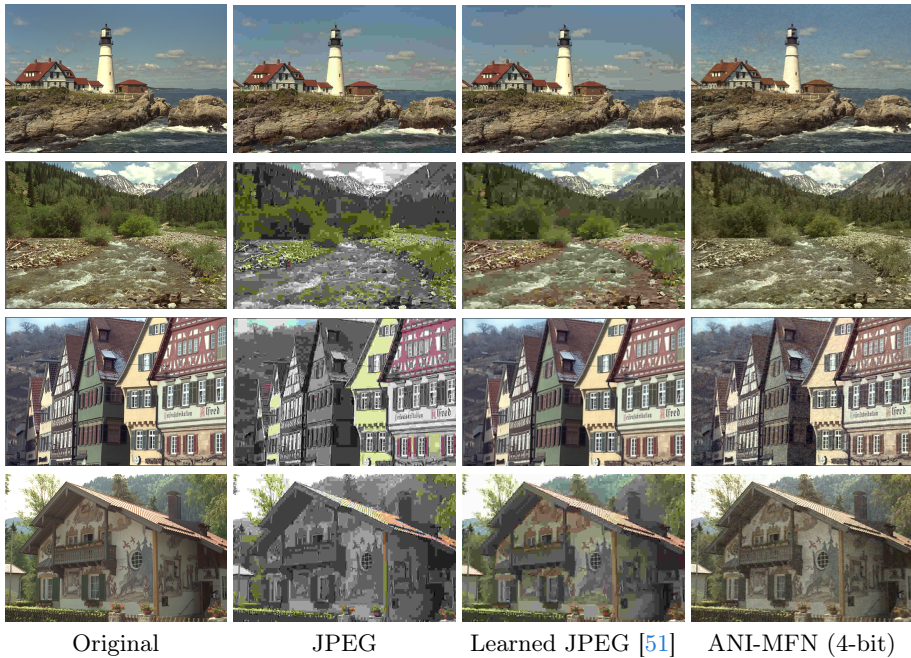


Fig. 14: Comparison with traditional codecs. Our proposed neural image ANI (at 4-bits) achieves high-fidelity results without clearly unpleasant artifacts. Note that all the images are around 0.3 bpp. The images from the Kodak dataset are: 13 and 24.